



LAWRENCE
LIVERMORE
NATIONAL
LABORATORY

Simulated performance of the optical Thomson scattering diagnostic designed for the National Ignition Facility

J. S. Ross, P. Datte, L. Divol, J. Galbraith, D. H. Froula, S. Glenzer, B. Hatch, J. Katz, J. Kilkenny, O. Landen, A. M. Manuel, W. Molander, D. S. Montgomery, J. D. Moody, G. Swadling, J. Weaver

June 8, 2016

HTPD 2016

Madison, WI, United States

June 5, 2016 through June 9, 2016

Disclaimer

This document was prepared as an account of work sponsored by an agency of the United States government. Neither the United States government nor Lawrence Livermore National Security, LLC, nor any of their employees makes any warranty, expressed or implied, or assumes any legal liability or responsibility for the accuracy, completeness, or usefulness of any information, apparatus, product, or process disclosed, or represents that its use would not infringe privately owned rights. Reference herein to any specific commercial product, process, or service by trade name, trademark, manufacturer, or otherwise does not necessarily constitute or imply its endorsement, recommendation, or favoring by the United States government or Lawrence Livermore National Security, LLC. The views and opinions of authors expressed herein do not necessarily state or reflect those of the United States government or Lawrence Livermore National Security, LLC, and shall not be used for advertising or product endorsement purposes.

Simulated performance of the optical Thomson scattering diagnostic designed for the National Ignition Facility^{a)}

J. S. Ross,¹ P. Datte,¹ L. Divol,¹ J. Galbraith,¹ D. H. Froula,² S. Glenzer,³ B. Hatch,¹ J. Katz,² J. Kilkenny,⁴ O. Landen,¹ A. M. Manuel,¹ W. Molander,¹ D. S. Montgomery,⁵ J. D. Moody,¹ G. Swadling,¹ and J. Weaver⁶

¹⁾Lawrence Livermore National Laboratory, Livermore, California 94551^{b)}

²⁾Laboratory for Laser Energetics, University of Rochester, Rochester, New York, USA

³⁾SLAC National Accelerator Laboratory, Menlo Park, California, USA

⁴⁾General Atomics, San Diego, CA 92186

⁵⁾Los Alamos National Laboratory, Los Alamos, New Mexico, USA

⁶⁾Plasma Physics Division, Naval Research Laboratory, Washington DC, USA

An optical Thomson scattering diagnostic has been designed for the National Ignition Facility (NIF) to characterize underdense plasmas. We report on the design of the system and the expected performance for different target configurations. The diagnostic is designed to spatially and temporally resolve the Thomson scattered light from laser driven targets. The diagnostic will collect scattered light from a 50-micron cubic volume. The system design allows operation with different probe laser wavelengths. A deep-UV probe beam ($\lambda_0 = 210$ nm) will be used to Thomson scatter from electron plasma densities of $\sim 5 \times 10^{20}$ cm⁻³ while a 3ω probe will be used for plasma densities of $\sim 1 \times 10^{19}$ cm⁻³. The system is designed to field two spectrometers: the first to resolve Thomson scattering from ion acoustic waves fluctuations and the second to resolve scattering from electron plasma wave fluctuations. Expected signal levels relative to background will be presented for typical target configurations (Hohlraums, planar foils, etc).

I. INTRODUCTION

An optical Thomson scattering (OTS) diagnostic has been designed for the National Ignition Facility (NIF) to characterize under dense plasma conditions in inertial confinement fusion (ICF) hohlraums¹. Based on expected background levels from Bremsstrahlung², stimulated scattering³, and Thomson scattering from the 3ω (351 nm) drive beams a 10 GW, 5ω (210 nm) probe laser with a 1 ns pulse length is being developed. This probe intensity will allow accurate measurements of the electron temperature and density for a range of target configurations. A 3ω beam can also be used as the Thomson scattering probe for lower density, lower background targets. A series of experiments are planned for the commissioning of the OTS diagnostic and the expected signals with a description of the methodology used to generate them are presented below.

The primary measurement of interest is the Thomson scattered signal with power scattered into a unit solid angle $d\Omega$ and a unit scattered frequency $d\omega_s$ given by⁴,

$$P_s d\Omega d\omega_s = \frac{P_i r_0^2}{A} d\Omega \frac{d\omega_s}{2\pi} n_e S(\mathbf{k}, \omega) G(\mathbf{k}, \omega), \quad (1)$$

where P_i is the incident power, A is the cross-sectional area of the Thomson-scattering volume, r_0 is the classical electron radius, n_e is the electron density, $S(\mathbf{k}, \omega)$ is the

spectral density function, and $G(\mathbf{k}, \omega)$ is a geometrical factor. The Thomson-scattering spectral density function is,

$$S(\mathbf{k}, \omega) = \frac{2\pi}{k} \left| 1 - \frac{\chi_e}{\varepsilon} \right|^2 f_{e0} \left(\frac{\omega}{k} \right) + \frac{2\pi Z}{k} \left| \frac{\chi_e}{\varepsilon} \right|^2 f_{i0} \left(\frac{\omega}{k} \right), \quad (2)$$

where $\varepsilon = 1 + \chi_e + \chi_i$ is the dielectric function, χ_e is the electron susceptibility, χ_i is the ion susceptibility, Z is the average ionization state, $\omega = \omega_s - \omega_i$, ω_s is the scattered frequency, ω_i is the incident frequency and $f_{e0}(\frac{\omega}{k})$ and $f_{i0}(\frac{\omega}{k})$ are the distributions for electrons and ions respectively.

The geometrical factor⁴ accounts for the electromagnetic interactions with the plasma. The geometric factor becomes unity in the “non-relativistic” limit when collection of the scattered light is normal to the direction of the laser beam polarization ($|\hat{k}_s \times (\hat{k}_s \times \hat{E}_i)|^2 = 1$). When ignoring terms of order $(v/c)^2$ and greater the geometrical factor becomes,

$$G(\mathbf{k}, \omega) = \left(1 + \frac{2\omega}{\omega_i} \right). \quad (3)$$

This first order correction term⁵ becomes relevant in the electron plasma wave feature as the plasma density increases.

Bremsstrahlung emission from the plasma is an expected source of background and has been estimated using the following formula²,

$$I_{B,\Omega,\lambda} = 10^{-7} \frac{16}{3} \left(\frac{\pi}{6m_e^3} \right)^{\frac{1}{2}} \frac{e^6}{c^2} \frac{Z n_e^2}{(k_B T_e)^{\frac{1}{2}}} \frac{1}{\lambda^2} \exp \left(\frac{hc}{\lambda k_B T_e} \right), \quad (4)$$

^{a)}Contributed paper published as part of the Proceedings of the 21th Topical Conference on High-Temperature Plasma Diagnostics, Madison, Wisconsin, June, 2016.

^{b)}Electronic mail: ross36@llnl.gov

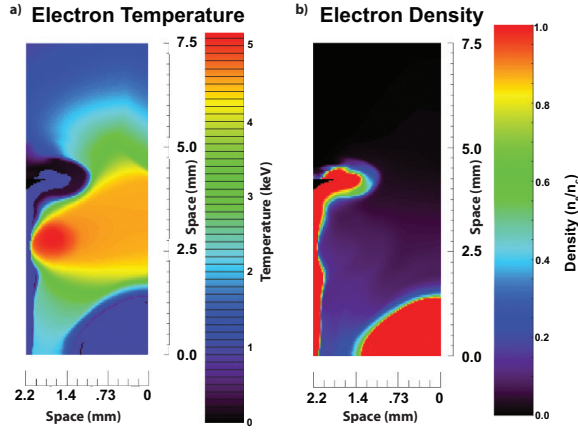


FIG. 1. (Color online) Cylindrically symmetric simulated hohlraum plasma conditions at peak laser power are shown. a) The electron temperature in keV and b) the electron density as a fraction of critical density for 3ω . The lower right corner is the capsule center and target chamber center. The high density, low temperature region at (2.2, 0) to (2.2, 4.5) is the hohlraum wall.

in units of $[\text{W cm}^{-3} \text{sr}^{-1} \text{nm}^{-1}]$ where m_e is the electron mass, c is the speed of light, T_e is the electron temperature, k_B is the boltzman constant, h is the Planck constant, and λ is the wavelength of the emitted radiation. The Bremsstrahlung emission is unpolarized while the Thomson scattering signal is polarized. A polarizer will be used to preferentially reject the Bremsstrahlung reducing its scattered power by 50%.

Simulated plasma conditions for each target configuration are used to generate the expected Thomson scattering signal and background. The electron temperature and electron density for an ICF hohlraum⁶ at peak laser intensity is shown in Figure 1. The Thomson scattering signal is calculated from the region the collection system and the 5ω probe beam overlap. The collect system is designed with a 50 micron collect aperture at the Thomson scattering volume. The probe beam will have a 50 micron diameter spot at best focus and will be collected in a nearly backscattered configuration producing a Thomson scattering angle of 169 degrees. The background is calculated for the collection cone of the diagnostic.

The collected signals, one resolving the electron plasma wave (EPW) feature and one resolving the ion-acoustic wave (IAW) feature, are modified by the system transmission as a function of wavelength as well as the quantum efficiency of streak camera. The gain of the system is used to generate the expected counts per pixel shown in Figure 2. The IAW signal is delayed approximately 5 ns relative to the EPW signal due to the differing path lengths of the spectrometers in the collection system. The Bremsstrahlung emission is collected by both systems, but dominated by the EPW channel due to the significantly larger wavelength range collected. The plasma conditions are assumed to be constant in time to simplify the calculation.

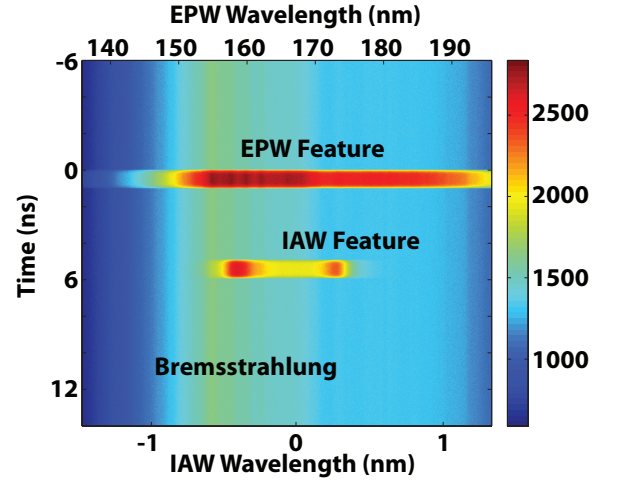


FIG. 2. (Color online) The synthetic experimental data from a hohlraum is shown. The scattered signals from two spectrometers are multiplex in time onto the streak camera entrance slit. The plasma conditions are assumed to be constant in time.

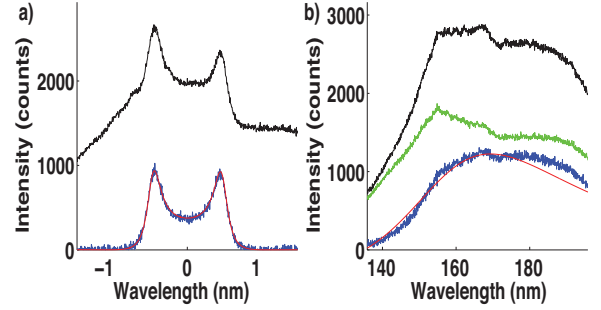


FIG. 3. (Color online) Lineouts of the expected signal are shown for the a) ion feature and b) electron feature. The ion feature background is dominated by background from the electron feature spectrometer due to the multiplexing of the signals. The measured signal (black line) is compared to the background (green line). The background subtracted signal (blue line) is compared to the ideal Thomson scattering spectra (red line).

Lineouts of the synthetic hohlraum data are shown in Figure 3. The IAW feature [Fig. 3 (a)] and the EPW feature [Fig. 3 (b)] are compared to the background and an ideal Thomson spectra. A signal to background ratio of 0.8 is expected when using a neutral density filter to reduce the overall signal by 10^{-2} . The spectral shape of the bremsstrahlung emission is dominated by the wavelength sensitivity of the collection system which is similar between 200 and 160 nm and then decreases rapidly below 150 nm.

The initial OTS commissioning experiments will include simple foil targets optimized for a 3ω probe laser. An example of the expected data is shown in Figure 4. This calculation uses a 3ω probe beam with a scattering angle of 130 degrees and a standard NIF phase plate

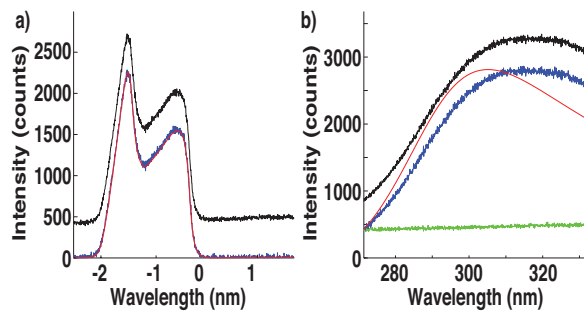


FIG. 4. (Color online) Lineouts of the expected signal are shown for the a) ion feature and b) electron feature. The ion feature background is dominated by background from the electron feature spectrometer due to the multiplexing of the signals. The measured signal (black line) is compared to the background (green line). The background subtracted signal (blue line) is compared to the ideal Thomson scattering spectra (red line).

with a focal spot diameter of 1.2 mm. This increases the size of the Thomson scattering volume relative to the 5ω probe configuration by approximately 5x in length. This increase in Thomson scattering volume size means that scattering from different electron densities and plasma flow velocities will be collected and is the primary reason for the asymmetry and width of the IAW feature in Fig. 4 (a). The discrepancy between the ideal Thomson spectra and the background subtracted signal is due to the

non-uniformity of the spectra response over the 270 to 330 nm wavelength range. The collect system has been optimized for the 5ω wavelength range between 160 to 210 nm.

In conclusion, a Thomson scattering diagnostic has been developed for the National Ignition Facility to characterize plasma conditions inside ICF hohlraums. A 10 GW, 5ω probe beam will be used to avoid background generated by the 3ω drive beams and bremsstrahlung emission. For targets with a lower background level a 3ω probe beam could also be used. Initial experiments with the collect system are planned at the end of 2016 with deployment of the 5ω probe beam expected in 2018.

This work was performed under the auspices of the U.S. Department of Energy by Lawrence Livermore National Laboratory under Contract DE-AC52-07NA27344.

- ¹J. D. Lindl, L. J. Atherton, P. A. Amendt, S. Batha, P. Bell, R. L. Berger, R. Betti, D. L. Bleuel, T. R. Boehly, D. K. Bradley, et al., *Nuclear Fusion* **51**, (2011).
- ²A. H. Gabriel, G. B. F. Niblett, and N. J. Peacock, *Journal Of Quantitative Spectroscopy & Radiative Transfer* **2**, 491 (1962).
- ³J. D. Moody, P. Datte, K. Krauter, E. Bond, P. A. Michel, S. H. Glenzer, L. Divol, C. Niemann, L. Suter, N. Meezan, et al., *Review Of Scientific Instruments* **81**, 10D921 (2010).
- ⁴D. H. Froula, J. Sheffield, and S. H. Glenzer, *Plasma Scattering of Electromagnetic Radiation, Theory and Measurement Techniques* (Academic Press, 2010).
- ⁵J. S. Ross, S. H. Glenzer, J. P. Palastro, B. B. Pollock, D. Price, L. Divol, G. R. Tynan, and D. H. Froula, *Physical Review Letters* **104**, (2010).
- ⁶O. S. Jones, C. J. Cerjan, M. M. Marinak, J. L. Milovich, H. F. Robey, P. T. Springer, L. R. Benedetti, D. L. Bleuel, E. J. Bond, D. K. Bradley, et al., *Physics Of Plasmas* **19**, 056315 (2012).